MANGANESE DIOXIDE DECORATED CARBON AEROGEL/CARBON FIBRE COMPOSITE AS A PROMISING ELECTRODE FOR STRUCTURAL SUPERCAPACITORS

E. A. Senokos[1], D. B. Anthony[1,2], S. N. Nguyen[2], A. R. Kucernak[1], E. S. Greenhalgh[2] and M. S. P. Shaffer[1,3*]

[1] Department of Chemistry, Imperial College London, UK
[2] Department of Aeronautics, Imperial College London, UK
[3] Department of Materials, Imperial College London, UK
* Corresponding author (m.shaffer@imperial.ac.uk)

Keywords: Carbon fibre, Manganese dioxide, Hybrid electrodes, Structural power composites

ABSTRACT

Manganese dioxide electrochemically deposited onto carbon aerogel/carbon fibres (CAG/CF) shows a great potential as an electrode material in multifunctional structural supercapacitors. MnO_2 nanowires grown by a pulse potentiometric method provide a large enhancement in capacitive performance of the carbon electrodes and symmetric supercapacitor devices based on the hybrid material.

1 INTRODUCTION

Multifunctional energy storage systems are able to retain their primary electrochemical functions but with significant structural mechanical integrity. By achieving a suitable balance between electrochemical and mechanical properties, such systems could deliver high power while acting as a load bearing structural element, potentially offering a weight reduction relative to monofunctional systems used in aerospace, electric/hybrid ground transport, and portable electronics.

Carbon fibres (CFs) are a primary reinforcing element in structural composites, widely used owing to their excellent mechanical performance. However, the low intrinsic specific surface area (SSA <1 m^2/g) limits their utilization for multifunctional structural supercapacitors. There is a central challenge to improve the electrochemical properties of structural carbon fibres, whilst avoiding degradation of their mechanical performance. Previously, various methods were explored to increase SSA without compromising mechanical and electrical properties [1], [2]. The most promising strategy, so far, is based on embedding structural carbon fibres into a monolithic carbon aerogel (CAG). Highly porous CAG-modified carbon fibre fabrics demonstrate a notable increase in capacitance from 0.06 F/g to 14.3 F/g, whilst offering promising mechanical characteristics [3]. Despite this success, further improvements in the CAG/CF composite electrodes are required in order to reach the level of multifunctional efficiency at which structural power devices offer a weight saving.

One strategy involves the deposition of pseudocapacitive materials (e.g. transition metal oxides or conducting polymers) which possess large charge-storage capacity resulting from fast and reversible surface-confined Faradaic reactions [4], [5]. This approach utilizes the CF/CAG carbon material as a highly porous conductive scaffold, which maximizes the effective surface of the redox active material and provides the channels for fast charge transport [6], [7].

In this work, we report the use of CAG-modified CFs as high surface area conductive structure for electrochemical deposition of pseudocapacitive manganese dioxide (MnO_2). The incorporation of MnO_2 leads to a hybrid composite electrode offering significant contribution of redox reactions to the charge storage mechanism, thus enhancing the total capacitance of the system. Optimization of deposition conditions allows the morphology and mass loading of metal oxide to be adjusted, resulting in a homogeneous distribution of MnO_2 with potentially high surface area exposed to electrolyte. The improvement in electrochemical performance of MnO_2@CAG/CF electrodes is evaluated in 2- and 3-electrode cells by electrochemical impedance spectroscopy, cyclic voltammetry and charge-discharge tests.

2 EXPERIMENTAL SECTION

2.1 Materials

Spread tow CF fabric (43 PW HS40 TeXtreme®, Oxeon AB) was used as the starting electrode material and as a structural scaffold for CAG. Resorcinol (≥99%), formaldehyde (37 wt.% solution in H_2O) and potassium hydroxide (≥85% KOH basis) used for CAG synthesis were purchased from Sigma Aldrich. Manganese(II) acetate tetrahydrate (≥99.0%) and sodium acetate (≥99.0%) used for electrochemical deposition of manganese oxide were obtained from Sigma Aldrich. All purchased chemicals were used as-received.

2.2 Fabrication of CAG-modified CF fabrics

CF fabrics were embedded within a CAG monolith by the method described previously [3]. Briefly, resorcinol-formaldehyde (RF) gel was formed by mixing R (resorcinol), F (formaldehyde) and KOH catalyst (C) in distilled water at molar ratios of R/F = 0.5 and R/C = 50 and overall RF weight fraction of 40 wt.%. After thorough stirring at 20 ˚C for 3 hours, and at 30 ˚C for 3 hours, the tightly sealed solution was kept at 5 ˚C for 24 hours. As-obtained RF polymer precursor was infused into CF fabrics by resin infusion under flexible tooling (RIFT) process. In short, CF were sealed within a RIFT plastic bag which was evacuated and permitted the uptake of RF sol throughout the fabric. The infused RF gel was polymerized at room temperature, 50 ˚C and 90 ˚C for 24 h at each temperature and left to dry at room temperature over 3 days. The dried RF/CF fabrics were then pyrolyzed at 800 ˚C under N_2 gas to produce CAG/CF samples.

2.3 Electrochemical deposition of MnO_2

MnO_2 nanostructures were deposited onto carbon fibre-based electrodes by electrochemical method. As-produced CAF/CF samples (~ 4 cm^2) were employed as the working electrodes using saturated calomel electrode (SCE) and platinum mesh as reference and counter electrodes, respectively. MnO_2 was coated onto CAG/CF by anodic electrodeposition through a pulse potentiometry. A pulse profile consisted of a current step of 200 mA/g applied for 10 ms followed by a 100 ms step of open-circuit voltage (OCV). The total “on” deposition time was set to 60 minutes equal to 360 000 pulse cycles. The precursor deposition solution contained 0.1M $MnAc_2$ and 0.1M NaAc dissolved in a mixture of ethanol and distilled water with a volumetric ratio of 1:1. The obtained MnO_2@CAG/CF composites were repeatedly rinsed with de-ionized water and dried at 70 ˚C under vacuum for 24 hours.

2.4 Microstructure characterization of MnO_2 coated CAG/CF fabrics

Morphology of the samples was characterised by scanning electron microscopy (Zeiss Auriga Cross Beam Workstation) operating at 5 kV. The crystal structure of the samples was analysed from X-Ray diffraction patterns obtained on a PANalytical Empyrean diffractometer with Cu K_α radiation (λ = 0.154 nm) at a generator voltage of 40 kV and an emission current of 40 mA.

2.5 Electrochemical characterization

Electrochemical performance of as-produced CAG/CF and MnO_2@CAG/CF samples was studied by cyclic voltammetry (CV) using a Biologic VMP potentiostatic–galvanostatic system and three-electrode cell configuration with SCE and Pt mesh as reference and counter electrodes, respectively. 1M Na_2SO_4 aqueous solution was used as the electrolyte. Scan rates applied ranged from 5 to 400 mV/s and the voltage window was fixed between -0.2V and +0.8V vs SCE. Specific capacitance was obtained by integrating the area under CV curves and normalizing by the weight of electrode material including CFs, CAG and MnO_2.

Full cell symmetric devices were assembled by sandwiching a cellulose paper separator between two carbon electrodes impregnated with 1M Na_2SO_4 electrolyte in a two-electrode Swagelok cell. Galvanostatic charge–discharge (CD) test at different current densities (1–20 mA cm^{-2}) and

Electrochemical Impedance Spectroscopy (EIS) with the frequency range varied from 200 kHz to 10 mHz were applied to study electrochemical performance of CAG/CF and MnO_2@CAG/CF electrodes in a full cell. Capacitance of the device was calculated from the slope of the discharge curve as C_{cell} = I/slope. Specific capacitance of a single electrode in a symmetric cell can be obtained as $C_s = 4C_{cell}$. The values of real energy and power densities were estimated according to the following equations:

$$E_{real} = I \int V dt \quad (1)$$

$$P_{real} = E_{real}/t_{dis} \quad (2)$$

where I is the current applied, V is the voltage window and t_{dis} is the discharge time.

3 RESULTS AND DISCUSSION

Various synthetic routes and organic precursors can be applied to produce high surface area carbon aerogel. RF gel-based carbons are considered as one of the most promising candidates due to their attractive properties including high electrical conductivity, controllable pore structures and high surface areas [8]–[10]. Thus, RF polymer precursor was chosen for infusion into CF fabrics and formation of CAG/CF composites. The premixed RF solution was infused into CF under vacuum according to a standard RIFT procedure, following by the subsequent gelation and curing of the gel. In order to obtain high surface area CAG as-produced organic gel was further carbonized under inert conditions.

The morphology of as-produced CAG/CF composite is shown in Figure 1a,b. A compact and thin CAG coating on CF spread tow (Figure 1a) confirms an effectiveness of the vacuum assisted infusion of RF precursor. Owing to good impregnation of RF sol into CF fabrics and mitigated formation of thick CAG skin the total weight fraction of CAG did not exceed 29 wt.%. SEM observation (Figure 1b) reveals highly porous CAG network consisting of mesopore channels of different size which is in

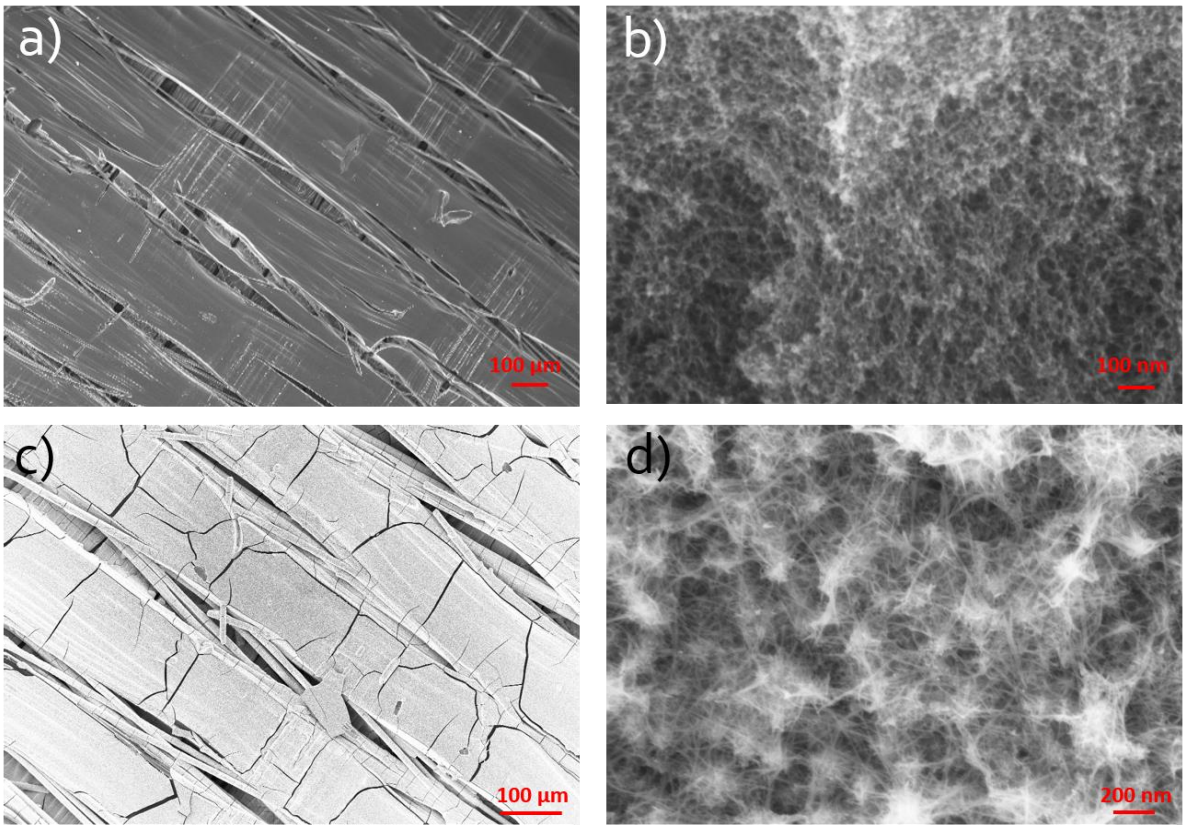

Figure 1: SEM images showing the morphology of (a, b) as-produced CAG/CF composite and (c, d) MnO_2 coated CAG/CF sample.

good accordance with our previous reports [3]. The resulting specific surface area of the composite obtained from BET (Brunauer–Emmett–Teller) analysis of N_2 adsorption–desorption isotherm corresponds to ~240 m^2/g. The porous character of the carbon electrode with suitable mesoporosity is an essential criterion for facile electrolyte infiltration into CAG required to form a large efficient capacitive surface and to enable more evenly distributed nanoparticles coating.

Pulse potentiometric electrodeposition was employed to deposit MnO_2 on CAG/CF fabrics. The pulse technique allows electrolyte ions to diffuse into the interior of CAG network thus avoiding a possible blockage of the pores. Whereas the diffusion rate of Mn^{2+} is a limiting factor of MnO_2 deposition, the longer OCV intervals enable penetration of the species farther into CAG pores and short current pulses confine nucleation and growth of the metal oxide. The anodic deposition of manganese dioxide in neutral supporting electrolytes occurs through a number of intermediate steps, involving electrochemical oxidation of Mn^{2+} to M^{3+}, hydrolysis of Mn^{3+} to MnOOH and its further electrochemical oxidation to MnO_2 [11]. The kinetics of these reactions depend on the deposition parameters (i.e. peak current density, duty cycle, deposition time) and determine both the microstructure of the oxide and efficiency of the coating. In this work, the pulse characteristics were chosen from the perspective of a preliminary optimization of the process which can be further tailored to achieve an optimum performance of the material.

SEM observation (Figure 1c) indicates that CAG is entirely coated with MnO_2 nanoparticles after 60 minutes of total time at peak current. It is clearly seen that MnO_2 is uniformly distributed all around the CAG and CF surface. Cracks detected on the surface of metal oxide layer are expected to be induced by shrinkage stress during drying which can be further prevented through controlled drying processes. SEM image at higher magnification (Figure 1d) reveals that MnO_2 nanoparticles consist of interconnected nanowires with a wide range of lengths and diameters forming a porous network of active material.

X-ray diffraction was further applied to investigate the crystal structure of the samples as it is known to impact electrochemical behaviour of the oxide [12]. Figure 2 shows XRD patterns obtained for as-produced and MnO_2 coated CAG/CF samples. The results indicate that two diffraction peaks clearly emerged after electrodeposition: a peak at a 2θ of 36.9° and a low intense peak at around 66.1°. Despite low signal-to-noise ratio denoting poor crystallinity of the produced MnO_2 the crystal structure of hexagonal akhtenskite ε-MnO2 still can be well defined (JCPDS no. 00-030-0820) [13]–[15].

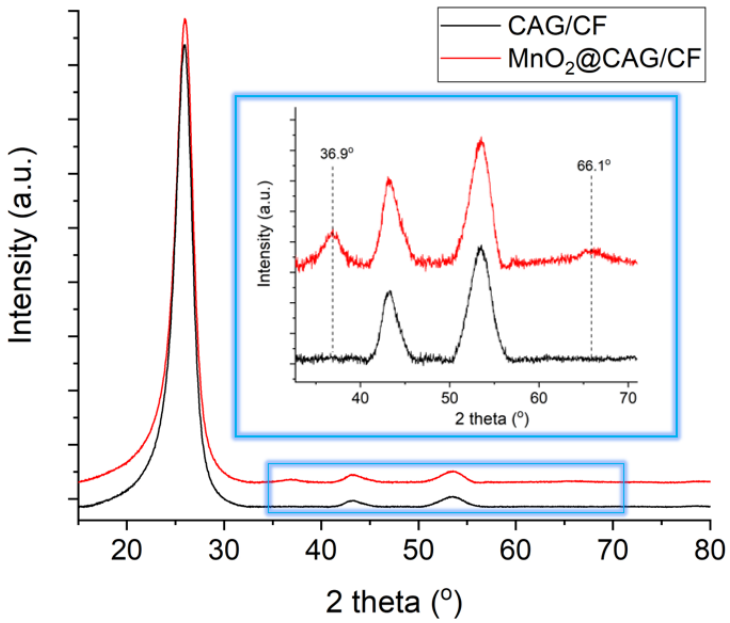

Figure 2: XRD profiles obtained for as-produced and MnO_2 modified (60 min deposition) CAG/CF samples.

Electrochemical properties of MnO_2-modified electrodes were studied and compared to as-produced CAG/CF fabrics by cyclic voltammetry in half-cell configuration in neutral 1M Na_2SO_4 aqueous electrolyte. Figure 3a depicts CV curves of the hybrid electrodes measured at different scan rates. At low scan rates CV plots demonstrate a quasi-rectangular shape with no peaks within the experimental electrochemical window which indicates that the hybrid electrode is charged and discharged at a pseudo-constant rate over the complete voltammetric cycle [16], [17]. As the scan rate increases, the peak current raises, while the shape of the curve deviates from the quasi-rectangular. This is associated to a limited mass transport of MnO_2 at faster voltage sweep. Cyclic voltammograms in Figure 3b compare capacitive properties of as-produced CAG/CF and the hybrid samples decorated with the metal oxide. The increased area under CV curve of MnO_2@CAG/CF electrode indicates a significant contribution of MnO_2 pseudocapacitance to total capacitive performance of the hybrid system. The corresponding values of specific capacitance estimated by integration of CV curves and normalised by the total mass of the electrodes are increased by almost 3 folds, reaching the maximum value of 53.6 F/g for the hybrid sample as compared to 18.6 F/g of as-produced CAG/CF. It is important to highlight that many reports on MnO_2-decorated materials describe electrochemical performance of the electrodes not considering contribution of current collector and necessary additives, resulting in overestimated capacitance not achievable in real SC devices. In contrast, MnO_2@CAG/CF poses a self-standing multifunctional electrode capable to be integrated into a full cell without additional components.

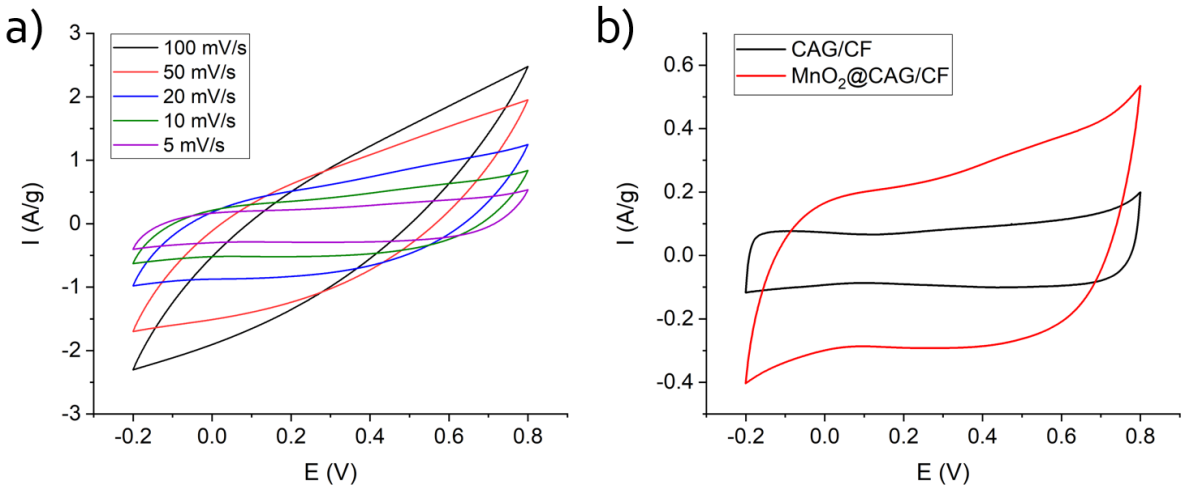

Figure 3. Electrochemical characterization in a half-cell in aqueous 1M Na_2SO_4 electrolyte: a) CV curves of MnO_2-decorated electrode at various scan rates and b) CV curves at 5 mV/s comparing capacitive performance of as-produced and MnO_2-modified CAG/CF fabrics.

In order to further evaluate electrochemical capabilities of the hybrid electrodes, a two-electrode symmetric device was assembled in a Swagelok cell and a series of CD tests were conducted at different current densities. Figure 4a depicts CD profiles obtained at 5 mA/cm^2 for CAG/CFs with and without MnO_2 coating. Triangular shape of the curves and high coulombic efficiency over 96% suggests fast and reversible Faradic reaction of MnO_2. The values of specific capacitance at different current densities obtained from discharge slopes are represented in Figure 4b. At low charge–discharge currents, capacitance of MnO_2@CAG/CF exhibits significant increase as compare to non-modified CAG/CF electrodes, achieving 47 F/g and 12.3 F/g, respectively, at high 1 mA/cm^2. At the same time, MnO_2@CAG/CF exhibits poor rate capability reflected in large decay of capacitance at higher current density. The decrease of capacitance with increasing scan rate is a common phenomenon for pseudocapacitive transition metal oxide associated to sluggish electron transport and hindered ion diffusion in a densely packed films [18]. This effect becomes more pronounced due to formation of excessive MnO_2 layer at the surface of CAG leading to a larger time constant for inter-particle pores [7], [19]. However, the drastic decrease of capacitance at high rates can be further improved by adjusting deposition conditions and additional post-synthetic treatments [20].

Ragone plot in Figure 4c illustrates an effect of MnO_2 deposition onto energy and power densities of SC device. As it is clear from the area under discharge curves in Figure 4a, symmetric SC based on hybrid electrodes demonstrates a noticeable increase of specific energy, reaching 1.66 Wh/kg which is 4 times larger than for CAG/CF (0.39 Wh/kg). Such a remarkable difference mainly arises from pseudocapacitive contribution of MnO_2, though possible improvement in hydrophilic behaviour of CAG/CF still should be considered. On the other hand, prolonged discharge time in CD curves associated to slow redox reaction of MnO_2 occurring over entire voltage window results in reduction of power density from 557 W/kg to 260 W/kg for as-produced and Mn coated CAG/CF, respectively.

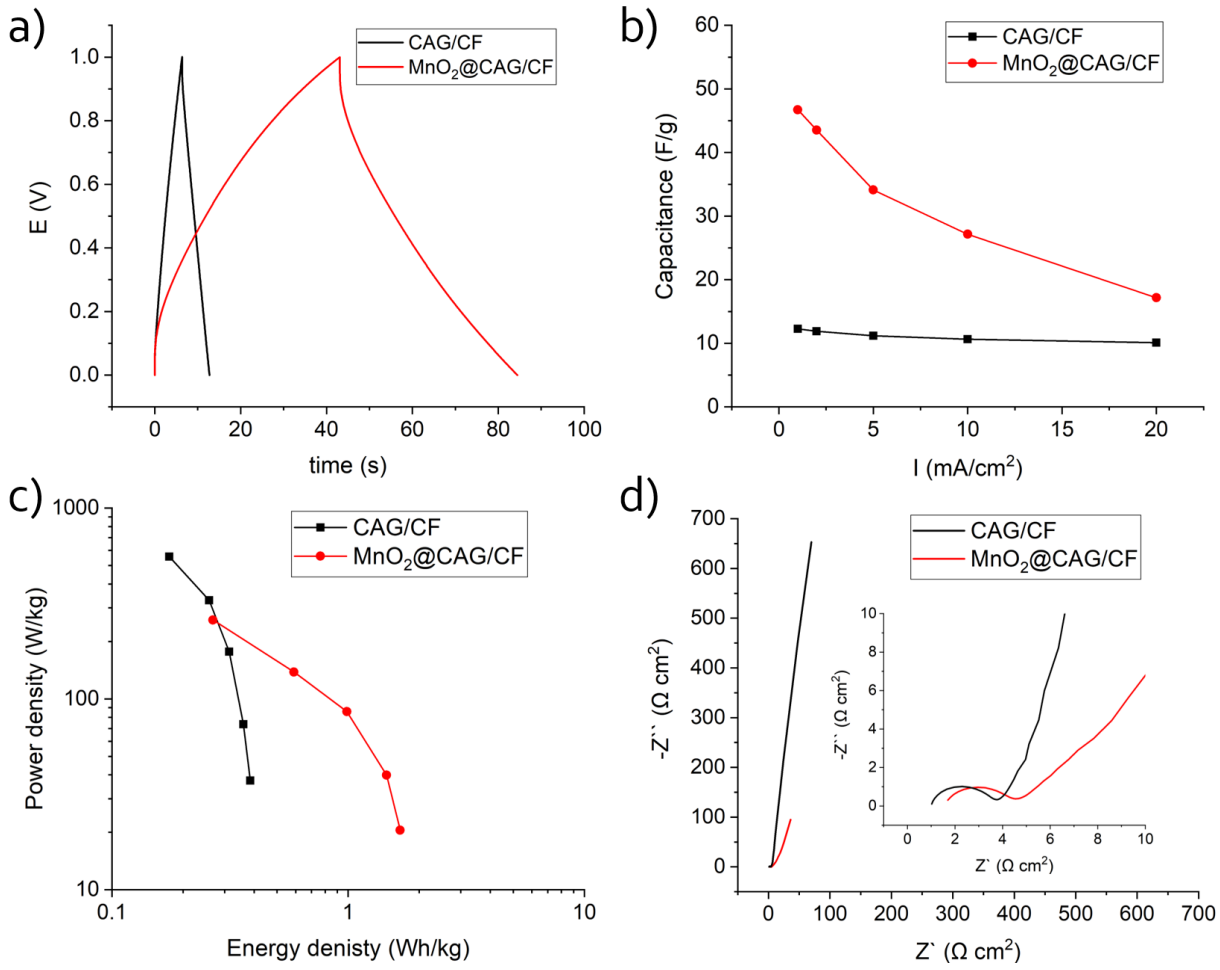

Figure 4. Electrochemical characterization in a symmetric full-cell in aqueous 1M Na_2SO_4 electrolyte: a) CD profiles, b) specific capacitance, c) Ragone and d) Nyquist plots comparing electrochemical performance of as-produced and MnO_2-modified CAG/CF fabrics in Swagelok cell.

Nyquist plots of the samples are displayed in Figure 4d. Both devices demonstrate typical resistive behaviour with well-defined semicircle in the low-frequency region. Apparently, equivalent series resistance (ESR) of MnO_2-coated material is 4.5 Ωcm^2, which is only 0.7 Ωcm^2 larger of that for as-produced CAG/CF (3.8 Ωcm^2). The slope of the Nyquist plot at mid frequency region clearly decreases after deposition of the metal oxide. Nearly vertical line for CAG-CF-based SC indicates a characteristic electric-double layer capacitive (EDLC) behaviour, while a 45° slope against the real axis for MnO_2-coated sample denotes a contribution of the Warburg resistance associated to semi-infinite diffusion processes observed for MnO_2-based electrodes [21], [22]. Finally, SC device based on hybrid electrode material exhibits substantially lower overall impedance which is inversely proportional to the total capacitance of the cell. This further confirms major contribution of MnO_2 to capacitive capabilities of the electrodes and hence a good prospect for its utilization in CAG/CF-based structural supercapacitors.

4 CONCLUSIONS

A facile electrochemical deposition method based on pulse potentiometry was applied to produce MnO_2 nanowires coated onto CAG/CF composite. Electrochemical properties of MnO_2@CAG/CF were evaluated in half and full cell and compared to as-produced CAG/CF fabrics. Symmetric SC device based on hybrid electrodes exhibits nearly 4 times increase of capacitance (47 F/g) and energy density (1.66 Wh/kg), while showing half the power density (260 W/kg). The study demonstrates a simple route to maximize capacitive performance of multifunctional structural supercapacitors which can be further tuned by adjusting the parameters of electrochemical deposition including deposition time, peak current density, duty cycle etc. Furthermore, in order to evaluate the prospect of MnO_2 coated electrodes for application in structural supercapacitors a part of the future work will be devoted to mechanical testing of the hybrid structures.

ACKNOWLEDGEMENTS

The authors would like to acknowledge the funding provided by the EPSRC Future Composites Research Manufacturing Hub (EP/P006701/1), the EPSRC Beyond Structural project (EP/P007465/1), the European Office of Aerospace Research and Development (IOE Grant FA9550-17-1-0251) and EU Clean Sky 2 (SORCERER Project #738085).

REFERENCES

[1] N. Shirshova *et al.*, Structural composite supercapacitors, *Composites Part A: Applied Science and Manufacturing*, **46**, 2013, pp. 96–107 (doi: 10.1016/j.compositesa.2012.10.007).

[2] L. E. Asp and E. S. Greenhalgh, Structural power composites, *Composites science and technology*, **101**, 2014, pp. 41–61 (doi: 10.1016/j.compscitech.2014.06.020).

[3] H. Qian, A. R. Kucernak, E. S. Greenhalgh, A. Bismarck, and M. S. P. Shaffer, Multifunctional Structural Supercapacitor Composites Based on Carbon Aerogel Modi fi ed High Performance Carbon Fiber Fabric, *ACS Appl. Mater. Interfaces*, **5**, 13, 2013, p. 6113 (doi: 10.1021/am400947j).

[4] Q. Cheng, J. Tang, J. Ma, H. Zhang, N. Shinya, and L.-C. Qin, Polyaniline-coated electro-etched carbon fiber cloth electrodes for supercapacitors, *The Journal of Physical Chemistry C*, **115**, 47, 2011, pp. 23584–23590 (doi: 10.1021/jp203852p).

[5] X. Zhao *et al.*, Rational design of polyaniline/MnO 2/carbon cloth ternary hybrids as electrodes for supercapacitors, *RSC Advances*, **5**, 81, 2015, pp. 66311–66317 (doi: 10.1039/C5RA10916G).

[6] J. Benson, I. Kovalenko, S. Boukhalfa, D. Lashmore, M. Sanghadasa, and G. Yushin, Multifunctional CNT-polymer composites for ultra-tough structural supercapacitors and desalination devices., *Advanced materials*, **25**, 45, 2013, pp. 6625–32 (doi: 10.1002/adma.201301317).

[7] A. Pendashteh, E. Senokos, J. Palma, M. Anderson, J. J. Vilatela, and R. Marcilla, Manganese dioxide decoration of macroscopic carbon nanotube fibers: From high-performance liquid-based to all-solid-state supercapacitors, *Journal of Power Sources*, **372**, 2017, pp. 64–73 (doi: 10.1016/j.jpowsour.2017.10.068).

[8] D. Wu, R. Fu, S. Zhang, M. S. Dresselhaus, and G. Dresselhaus, Preparation of low-density carbon aerogels by ambient pressure drying, *Carbon*, **42**, 10, 2004, pp. 2033–2039 (doi: 10.1016/j.carbon.2004.04.003).

[9] S.-J. Kim, S. W. Hwang, and S. H. Hyun, Preparation of carbon aerogel electrodes for supercapacitor and their electrochemical characteristics, *Journal of materials science*, **40**, 3, 2005, pp. 725–731 (doi: 10.1007/s10853-005-6313-x).

[10] A. M. ElKhatat and S. A. Al-Muhtaseb, Advances in tailoring resorcinol-formaldehyde organic and carbon gels, *Advanced materials*, **23**, 26, 2011, pp. 2887–2903 (doi: 10.1002/adma.201100283).

[11] M. Ghaemi and L. Binder, Effects of direct and pulse current on electrodeposition of manganese dioxide, *Journal of Power Sources*, **111**, 2, 2002, pp. 248–254 (doi:

10.1016/S0378-7753(02)00309-9).

[12] S. Devaraj and N. Munichandraiah, Effect of crystallographic structure of MnO2 on its electrochemical capacitance properties, *The Journal of Physical Chemistry C*, **112**, 11, 2008, pp. 4406–4417 (doi: 10.1021/jp7108785).

[13] E. Hayashi *et al.*, Effect of MnO2 Crystal Structure on Aerobic Oxidation of 5-Hydroxymethylfurfural to 2, 5-Furandicarboxylic Acid, *Journal of the American Chemical Society*, **141**, 2, 2019, pp. 890–900 (doi: 10.1021/jacs.8b09917).

[14] Y. Hao *et al.*, Manganese dioxide nanosheets-based redox/pH-responsive drug delivery system for cancer theranostic application, *International journal of nanomedicine*, **11**, 2016, p. 1759 (doi: 10.2147/IJN.S98832).

[15] D. Han, X. Jing, P. Xu, Y. Ding, and J. Liu, Facile synthesis of hierarchical hollow ε-MnO2 spheres and their application in supercapacitor electrodes, *Journal of Solid State Chemistry*, **218**, 2014, pp. 178–183 (doi: 10.1016/j.jssc.2014.06.041).

[16] S.-J. Bao, B.-L. He, Y.-Y. Liang, W.-J. Zhou, and H.-L. Li, Synthesis and electrochemical characterization of amorphous MnO2 for electrochemical capacitor, *Materials Science and Engineering: A*, **397**, 1–2, 2005, pp. 305–309 (doi: 10.1016/j.msea.2005.02.058).

[17] M. Xu, L. Kong, W. Zhou, and H. Li, Hydrothermal synthesis and pseudocapacitance properties of α-MnO2 hollow spheres and hollow urchins, *The Journal of Physical Chemistry C*, **111**, 51, 2007, pp. 19141–19147 (doi: 10.1021/jp076730b).

[18] Y. He *et al.*, Freestanding three-dimensional graphene/MnO2 composite networks as ultralight and flexible supercapacitor electrodes, *ACS nano*, **7**, 1, 2012, pp. 174–182 (doi: 10.1021/nn304833s).

[19] S. Yoon, J. H. Jang, H. K. Bok, and S. M. Oh, Complex capacitance analysis on rate capability of electric-double layer capacitor (EDLC) electrodes of different thickness, *Electrochimica Acta*, **50**, 11, 2005, pp. 2255–2262 (doi: 10.1016/j.electacta.2004.10.009).

[20] Y. Song *et al.*, Ostwald ripening improves rate capability of high mass loading manganese oxide for supercapacitors, *ACS Energy Letters*, **2**, 8, 2017, pp. 1752–1759 (doi: 10.1021/acsenergylett.7b00405).

[21] C. Wan, L. Yuan, and H. Shen, Effects of electrode mass-loading on the electrochemical properties of porous MnO2 for electrochemical supercapacitor, *Int. J. Electrochem. Sci*, **9**, 2014, pp. 4024–4038.

[22] H. R. Barai, A. N. Banerjee, N. Hamnabard, and S. W. Joo, Synthesis of amorphous manganese oxide nanoparticles–to–crystalline nanorods through a simple wet-chemical technique using K+ ions as a ‘growth director’and their morphology-controlled high performance supercapacitor applications, *RSC Advances*, **6**, 82, 2016, pp. 78887–78908 (doi: 10.1039/C6RA18811G).